ChemComm

Accepted Manuscript

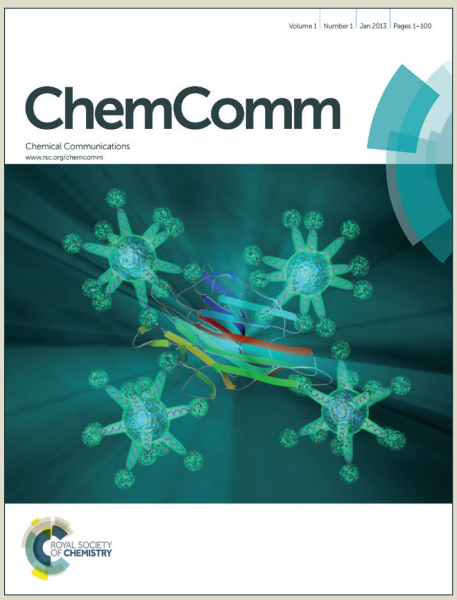

ROYAL SOCIETY OF CHEMISTRY

www.rsc.org/chemcomm

Journal Name

RSCPublishing

COMMUNICATION

Insights Into an Intriguing Gas Sorption Mechanism in a Polar Metal–Organic Framework with Open-Metal Sites and Narrow Channels

Cite this: DOI: 10.1039/x0xx00000x

Received 00th January 2012,
Accepted 00th January 2012

DOI: 10.1039/x0xx00000x

www.rsc.org/

Katherine A. Forrest,[a]†Tony Pham,[a]†Keith McLaughlin,[a]Adam Hogan[a] and Brian Space*[a]

Simulations of H_2 and CO_2 sorption were performed in the metal-organic framework (MOF), [Cu(Me-4py-trz-ia)]. This MOF was recently shown experimentally to exhibit high uptake for H_2 and CO_2 sorption and this was reproduced and elucidated through the simulations performed herein. Consistent with experiment, the theoretical isosteric heats of adsorption, Q_{st}, were nearly constant across all loadings for both sorbates. The simulations revealed that sorption directly onto the open-metal sites was not observed in this MOF, ostensibly a consequence of the low partial positive charges of the Cu^{2+} ions as determined through electronic structure calculations. Sorption was primarily observed between adjacent carboxylate oxygen atoms (site 1) and between nearby methyl groups (site 2) of the organic linker. In addition, saturation of the most energetically favorable sites (site 1) is possible only after filling a nearby site (site 2) first due to the MOF topology. This suggests that the lack of dependence on loading for the Q_{st} is due to the concurrent filling of sites 1 and 2, leading to an observed average Q_{st} value.

Metal–organic frameworks (MOFs) are porous materials that consists of metal ions coordinated to organic ligands to form a three–dimensional structure.[1] They have promising potential for a variety of energy-related applications, such as H_2 storage[2] and CO_2 capture and separation.[3] A variety of MOFs with different pore sizes, topologies, and chemical functionalities have been synthesized by simply tuning the metal ion and/or organic ligand.[4] MOFs that possess open-metal sites and/or narrow pore sizes have been shown to display increased affinity towards H_2 and CO_2.[5,6]

Recently, a MOF containing both open-metal sites and narrow pore sizes was synthesized and it was shown to exhibit high H_2 and CO_2 uptake through experimental measurements.[7] It is known as [Cu(Me-4py-trz-ia)] and consists of Cu^{2+} ions that are coordinated to Me-4py-trz-ia^{2-} ligands (Me-4py-trz-ia^{2-} = 5-(3-methyl-5-(pyridin-4-yl)-4*H*-1,2,4-triazol-4-yl)isophthalate) (Figure 1). The MOF contains two chemically distinct Cu^{2+} ions, with one ion coordinated to a carboxylate group and pyridine N atom of the linker (denoted as Cu1, see Figure S4) and the other coordinated to a carboxylate group and triazole N atom (denoted as Cu2, see Figure S4). Both Cu^{2+} ions represent a square planar 4-connected node for the tetradentate Me-4py-trz-ia^{2-} ligands, resulting in a MOF with platinum sulfide (**PtS**) topology.[8] This MOF undergoes several structural transitions upon activation which are dependent on the post–synthetic treatment used on the material. The Soxhlet extraction activated MOF is highly porous; the [Cu(Me-4py-trz-ia)] MOF activated is depicted in Figure 1. Note, different views of the MOF are provided in the Supporting Information.

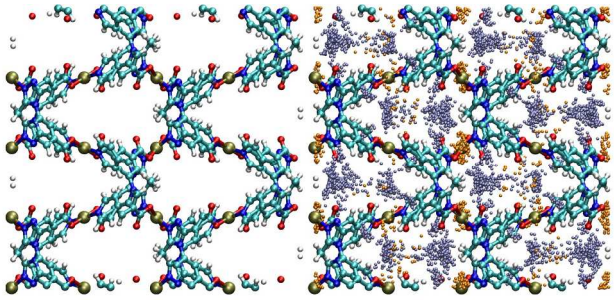

Fig. 1: The shifted *c* axis view of the 2 × 2 × 2 unit cell system of [Cu(Me-4py-trz-ia)]. (a) Empty; (b) Populated showing the locations of binding sites 1 (lavender) and 2 (orange). Note, site 2 does not correspond to sorption onto the Cu^{2+} ions, but between two adjacent methyl groups behind those ions. Atom colors: C = cyan, H = white, N = blue, O = red, Cu = tan.

Experimental studies have demonstrated that [Cu(Me-4py-trz-ia)] can sorb 15.2 mmol g^{-1} (3.07 wt %) of hydrogen at 77 K and 1.0 atm; this is currently the highest out of all MOFs reported thus far at this state point.[2,7] Further, the MOF is capable of sorbing 6.1 mmol g^{-1} (26.8 wt %) of CO_2 at 298 K and 1.0 atm, which is one of the highest among reported MOFs under these conditions.[3,7] Although [Cu(Me-4py-trz-ia)] has high uptake capacity for H_2 and CO_2, the initial isosteric heats of adsorption, $Q°_{st}$, values for these sorbates are interestingly lower than most MOFs that have large uptakes for the respective sorbates, with constant values of approximately 6.5 kJ mol^{-1} and 30.0 kJ mol^{-1} for H_2 and CO_2, respectively, across the loading range. Note, while the aforementioned $Q°_{st}$ values are ~~is~~ not as high as those for other highly sorbing MOFs, the values do not exhibit the typical monotonic decreasing behavior with increasing loading. As a result, we expect that this compound will exhibit some intriguing sorption properties that can be examined through molecular simulation studies. Thus, in this work, grand canonical Monte Carlo (GCMC) studies of H_2 and CO_2 sorption were performed in [Cu(Me-4py-trz-ia)] to investigate the gas sorption mechanism in the MOF.

GCMC simulations of H_2 and CO_2 sorption in [Cu(Me-4py-trz-ia)] were performed in a 2 × 2 × 2 unit cell system of the MOF as represented in Figure 1. More details of the GCMC methods used in this work, including a description of how certain thermodynamic quantities are calculated, can be found in the Supporting Information. The force field for [Cu(Me-4py-trz-ia)] includes repulsion/dispersion parameters, atomic point partial charges, and atomic point polarizabilities on the nuclear center of all atoms of the framework. An explanation of how these parameters were obtained is provided in the Supporting Information. The polarizability parameters were included to model explicit many-body polarization interactions, which was implemented using a Thole-Applequist type model (see Supporting Information).[9] Polarizable potentials for H_2[10] and CO_2[11] were used for the simulations in this work (see Supporting Information).

For the purpose of simulation, the MOF was treated as rigid. There was some question in the literature as to the validity of this assumption in this case.[7] To test our assumption, density functional theory (DFT) calculations using the Vienna *ab initio* Simulation Package (VASP)[12] with variable loadings of H_2 or CO_2 present in a unit cell of the MOF revealed that the material remains essentially unchanged with the sorbate molecules present in the pores for geometry optimization of the MOF–sorbate system. Further, the pore volume of [Cu(Me-4py-trz-ia)] was calculated using a simulation method involving helium (see Supporting Information),[13] and was found to be 0.591 cm^3 g^{-1}, which is in good agreement to the value obtained using the experimental N2 sorption isotherm at 77 K (0.586 cm^3 g^{-1}) and using the PLATON software (0.594 cm^3 g^{-1}).[14]

The simulated low-pressure excess H_2 sorption isotherms at 77 K, 87 K, and 97 K are in outstanding agreement with the corresponding experimental isotherms in [Cu(Me-4py-trz-ia)] (Figure S7). Note, all experimental data points were estimated from reference 7. The maximum calculated error is ±0.15 mmol

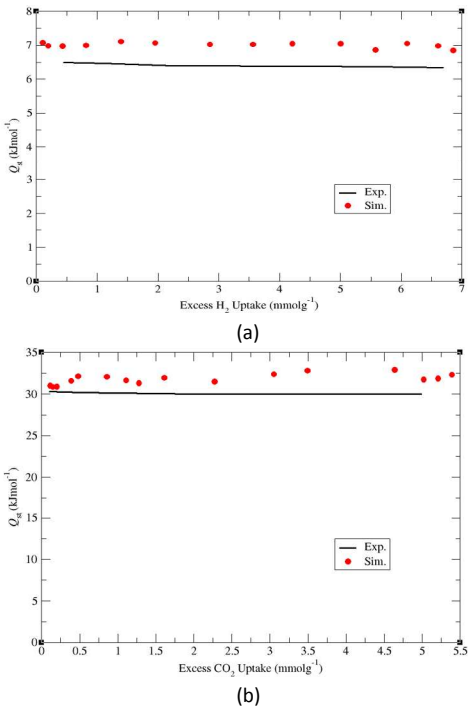

Fig. 2: Isosteric heats of adsorption, Q_{st}, for (a) H_2 and (b) CO_2 plotted against excess uptakes in [Cu(Me-4py-trz-ia)] for experiment (black line) and simulation (redcircles).

g^{-1} for the hydrogen modeling. At 77 K and 1.0 atm, the density of hydrogen in the pores of [Cu(Me-4py-trz-ia)] was calculated to be 0.052 g cm^{-3}, which is close to the density of liquid hydrogen (0.071 g cm^{-3}). The simulated H_2 sorption isotherm in [Cu(Me-4py-trz-ia)] at 77 K and higher pressures (up to 30.0 atm) is also in good agreement with experiment for the pressure range considered (Figure S8). The maximum calculated excess H_2 uptake was approximately 20.0 mmol g^{-1}, which is consistent with experimental measurements. The simulated CO_2 sorption isotherms at 273 K, 298 K, and 323 K are also in good agreement with the corresponding experimental data for pressures up to 40.0 atm (Figure S13). For CO_2, liquid-like density is reached when the MOF sorbs approximately 12.0 mmol g^{-1} of sorbate, which is captured at 273 K when the isotherm starts to saturate.

The GCMC-calculated Q_{st} values for both H_2 and CO_2 are shown in Figure 2 and are compared to those that were derived experimentally for the respective sorbates. As with the experimental values, the simulated Q_{st} values are relatively constant across all loadings for both sorbate molecules. This behavior in the Q_{st} values with increasing loading usually indicates little or no interaction with the open-metal sites and/or homogeneity within the binding sites of the material. Note, a small increase in the simulated Q_{st} values with increasing loading is noticeable for CO2 sorption at very low loadings. This implies that the CO_2 molecules are sorbing firstly to a site that is slightly less energetically favorable than another site.

Inspection of the radial distribution functions, g(*r*), of H_2 molecules about both chemically distinct Cu^{2+} ions in [Cu(Me-4py-trz-ia)] at 77 K and different pressures reveal that there is no

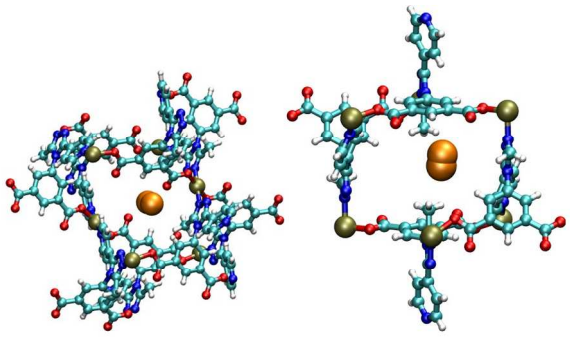

Fig. 3: Molecular illustration of a sorbed hydrogen molecule about (a) site 1 and (b) site 2 in [Cu(Me-4py-trz-ia)] as determined from simulation. The sorbate molecule is shown in orange. Note, orientational constraints are not imposed on the hydrogen molecule at the binding sites. Atom colors: C = cyan, H = white, N = blue, O = red, Cu = tan.

direct sorption onto either Cu^{2+} ions for all three pressures considered (Figure S9). Indeed, the closest Cu^{2+}–H_2 interaction occurs at approximately 3.5 Å, which is longer than a typical metal/hydrogen physisorption interaction distance. For instance, the distance between the center-of-mass of a sorbed hydrogen molecule and a Cu^{2+} ion of a copper paddlewheel unit, $[Cu_2(O_2CR)_4]$, was observed to be in the range of 2.39 to 2.50 Å.[15-16] In addition, the g(*r*) of hydrogen molecules are comparable across all pressures considered for the respective Cu^{2+} ions, which implies that the sorbate packing mechanism in this MOF is similar for all loadings.

Examination of the distribution of induced dipoles resulting from the polarizable potential for H_2 in [Cu(Me-4py-trz- ia)] at 77 K and various pressures reveal two distinct dipolar populations, with each peak correlating to a specific region of occupancy inside the MOF (Figure S10). The MOF causes hydrogen to behave as a weakly dipolar fluid. There are two different H_2 binding sites in [Cu(Me-4py-trz-ia)] as observed from the polarization distribution. The peak from 0.065 D to 0.20 D corresponds to occupancy within the region between two adjacent carboxylate oxygen atoms of the linker (site 1) (Figures 3(a) and S11(a)). For the peak ranging from 0.00 to 0.065 D, the hydrogen molecules with these dipole magnitudes were observed to sorb in the region between two adjacent methyl groups of the linker (site 2) (Figures 3(b) and S11(b)).

The energetics associated with both of the aforementioned binding sites are distinct from each other, with the binding energy being higher for site 1 (7.3 kJ mol^{-1} vs. 6.5 kJ mol^{-1} as determined from canonical Monte Carlo (CMC) simulations). The average value between the two binding sites for hydrogen is 6.9 kJ mol^{-1}, which is in good agreement with the Q_{st} values obtained from experiment and GCMC simulations. This suggests that the observed Q_{st} values for experiment and GCMC simulation are attributed to the concurrent filling of the two sites. The distance between the center-of-mass of the two H_2 molecules sorbed about sites 1 and 2, respectively, based on simulated annealing was observed to be 4.20 Å (Figure S12). From the normalized dipole distribution shown in Figure S10, it can be observed that the relative distribution of H_2 molecules sorbed about site 1 to site 2 is nearly 3:1 for all pressures considered.

The lack of a drop in the Q_{st} values as loading increases can be attributed to the fact that the more favorable site (site 1) cannot be accessed without sorbing onto the less favorable site (site 2) first, thus keeping the general ratio of occupancy even for all loadings. Indeed, as the hydrogen molecules are sorbed in this MOF, it must pass through the region between two methyl groups before it can occupy the region between two carboxylate oxygen atoms. While the region between the two methyl groups (site 2) exists in a side corridor off the channel shown in Figure 1 (containing the region between two adjacent carboxylate oxygen atoms (site 1)), the methyl group functionality projects into the channel and must be bypassed in order for the sorbate molecules to penetrate further into the crystal structure. This causes the sorbate molecules to sorb onto site 2 prior to proceeding to site 1 (Figure S3). This mechanism explains the MOF's sorbent capacity without a large Q_{st} and suggests a design principle for maximizing capacity while minimizing $Q°_{st}$, that is, good capture/storage with desirable kinetics.

The barrier height for the transition from site 2 to site 1 was calculated with the aid of molecular dynamics (MD) simulations and was found to be approximately 0.80 kJ mol^{-1} for H2 (Figure S19(a)). This value is appreciably small as it suggests that the hydrogen molecules can transit from site 2 to site 1 at the temperature considered (77 K), although the barrier is non-negligible and cooperative effects are not implausible. Note, within the pores of the material, the two sites have alternating locations within the narrow channels (i.e., site 2, site 1, site 2, etc). The alternation of the sorption sites presents a MOF design strategy where a highly favorable sorption site attracts a sorbate molecule while allowing the embedding of useful functionalities for the secondary site for applications such as molecular sieving.

An analogous sorption mechanism can be seen for CO_2 sorption in [Cu(Me-4py-trz-ia)]. The g(*r*) of CO_2 molecules about the two Cu^{2+} ions reveals no direct sorption onto the open-metal sites for all pressures (Figure S14). Moreover, the high dipole magnitude region in the dipole distribution for CO_2 in [Cu(Me-4py-trz-ia)] at different pressures (Figure S15) corresponds to sorption between two carboxylate oxygen atoms (Figures S16(a) and S17(a)), while the low dipole magnitude region corresponds to sorption between two methyl groups (Figures S16(b) and S17(b)). A distance of about 4.29 Å was measured between the carbon atoms of the two CO_2 molecules that are sorbed about sites 1 and 2 in the MOF based on positions that were determined through simulated annealing (Figure S18). Examination of the modeled system cell at CO_2 saturation revealed an approximately 4 to 1 distribution in favor of site 1.

The difference in the binding energy between the two sites for CO_2 was calculated to be 3.8 kJ mol^{-1} (site 1 = 32.0 kJ mol^{-1}; site 2 = 28.2 kJ mol^{-1}) and a barrier height of about 10.5 kJ mol^{-1} was estimated for the transition from site 2 to site 1 (Figure S19(b)). This barrier is significant but is clearly overcome in filling the sites under the conditions considered. As in the case of H_2, the average binding energy between the two sites for CO_2 (*ca.* 30 kJ mol^{-1}) is consistent with the CO_2 Q_{st} values for experiment

and GCMC simulation. Based on our results for H_2 and CO_2 sorption in [Cu(Me-4py-trz-ia)] and the similarities in the sorption mechanism between the two sorbates, the behavior towards different linear sorbates in this MOF seems to be "universal" in this sorbate size regime.

The absence of loading onto either Cu^{2+} ions for both sorbates in [Cu(Me-4py-trz-ia)] can be explained by the magnitudes of the partial charges for both ions. Electronic structure calculations on [Cu(Me-4py-trz-ia)] through fragment analysis reveal that the positive charges of both Cu^{2+} ions are quite low (see Tables S1 and S2). The Cu1 ion has a partial charge that is close to 0 e^-, while the Cu2 ion has a charge that is a little less than 0.5 e^-, which is still low com- pared to those for Cu^{2+} ions on copper paddlewheels. With the Cu1 ion coordinating to the pyridine N atom, there exists a π backbonding interaction between the two atoms in which the electrons from the pyridine group are donated to the empty orbitals of the Cu^{2+} ion. This causes the electron density of the Cu1 ion to increase significantly, which explains the very low positive charge for the Cu1 ion. A similar interaction exists between the Cu2 ion and the triazole N atoms, although there is lesser tendency for the triazole group to donate electrons to the Cu^{2+} ion compared to pyridine. Note, it was observed in previous simulation studies in MOFs with open-metal Cu^{2+} ions via copper paddlewheel clusters that a partial charge of 1.0 e^- or greater for the Cu^{2+} ion is required for sorption onto the open-metal sites with explicit polarization.[16]

In conclusion, GCMC simulations of H_2 and CO_2 sorption were performed for [Cu(Me-4py-trz-ia)], a MOF that has been shown to display very high uptake for the respective sorbates with modest $Q°_{st}$ values. Although explicit polarization was included in the simulations, direct sorption onto the open-metal sites was not observed. This is because the Cu^{2+} ions have low partial positive charges as a consequence of the electrostatic environment of the framework. There is not enough electron deficiency on the Cu^{2+} ions to motivate sorption onto those sites. The simulated Q_{st} values were observed to be nearly constant over the considered loading range for both sorbates, which agrees with experimental measurements. The results from the radial distribution functions about the Cu^{2+} ions and the dipole distribution for both sorbates indicate the absence of sorption onto either Cu^{2+} ion in [Cu(Me-4py-trz-ia)]. Thus, it appears that the sorption mechanism in this compound is not governed by metal–sorbate coordination, but rather the interaction between the sorbate molecules with the organic ligands within the small pores. Further, due to the geometric properties of the MOF, both sorption sites must be filled coincidentally, leading to virtually a constant Q_{st} value for all loadings considered.

The authors thank Jens Moellmer and Marcus Lange for providing a copy of reference 7, which inspired interest in modeling the MOF studied herein. The authors also thank Jens Bergmann for general discussions on this MOF. This work was supported by the National Science Foundation (Award No. CHE-1152362). Computations were performed under a XSEDE Grant (No. TG-DMR090028) to B.S. This publication is also based on work supported by Award No. FIC/2010/06, made by King Abdullah University of Science and Technology (KAUST). In addition, the author thank the Space Foundation (Basic and Applied Research) for partial support. Lastly, the authors would like to acknowledge the use of the services provided by Research Computing at the University of South Florida.

Notes and references

[a]Department of Chemistry, University of South Florida, 4202 East Fowler Avenue, CHE205, Tampa, FL 33620, USA. E-mail: brian.b.space@gmail.com

† Authors contributed equally.

Electronic Supplementary Information (ESI) available: Details of electronic structure calculations, grand canonical Monte Carlo methods, molecular dynamics simulations, and sorbate models, many-body polarization overview, pictures of MOF fragments, tables of properties, and additional H_2 and CO_2 sorption results. See DOI: 10.1039/c000000x/

1 O. M. Yaghi, H. Li, C. Davis, D. Richardson and T. L. Groy. *Acc. Chem. Res*., **1998**, *31*, 474.
2 M. P. Suh, H. J. Park, T. K. Prasad and D.-W. Lim. *Chem. Rev*.**2012**, *112*, 782.
3 K. Sumida, D. L. Rogow, J. A. Mason, T. M. McDonald, E. D. Bloch, Z. R. Herm, T.-H. Bae and J. R. Long. *Chem. Rev*. **2012**, *112*, 724.
4 M. Eddaoudi, D. B. Moler, H. Li., B. Chen, T. M. Reineke, M. O'Keeffe and O. M. Yaghi. *Acc. Chem. Res*., **2001**, *34*, 319.
5 P. D. C. Dietzel, P. A. Georgiev, J. Eckert, R. Blom, T. Strassle and T. Unruh. *Chem. Commun*., **2010**, *46*, 4962.
6 P. Nugent, Y. Belmabkhout, S. D. Burd, A. J. Cairns, R. Luebke, K. Forrest, T. Pham, S. Ma, B. Space, L. Wojtas, M. Eddaoudi and M. J. Zaworotko. *Nature,***2013**, *495*, 80.
7 D. Lässig, J. Lincke, J. Moellmer, C. Reichenbach, A. Moellmer, R. Glässer, G. Kalies, K. Cychosz, M. Thommes and R. Staudt. *Angew. Chem. Int. Ed*.,**2011**, *50*, 10344.
8 V. A. Blatov, A. P. Shevchenko and V. N. Serezhkin. *J. Appl. Crystallogr*., **2000**, *33*, 1193.
9 (a) J. Applequist, J. R. Carl and K.-K. Fung. *J. Am. Chem. Soc*., **1972**, *94*, 2952.; (b) B. Thole. *Chem. Phys*., **1981**, *59*, 341.; (c) K. A. Bode and J. Applequist. *J. Phys. Chem*., **1996**, *100*, 17820.
10 J. L. Belof, A. C. Stern and B. Space, *J. Chem. Theory Comput*., **2008**, *4*, 1332.
11 A. L. Mullen, T. Pham., K. A. Forrest, C. R. Cioce, K. McLaughlin and B. Space. *J. Chem. Theory Comput*., **2013**, *9*, 5421.
12 (a) G. Kresse and J. Hafner. *Phys. Rev. B*, **1993**, 47, 558.; (b) G. Kresse and J. Hafner. *Phys. Rev. B*, **1994**, *49*, 14251.; (c) G. Kresse and J. Furthmüller. *J. Comput. Mater. Sci*., **1996**, *6*, 15. (d) G. Kresse and J. Furthmüller. *Phys. Rev. B*, **1996**, *54*, 11169.
13 O. Talu and A. L. Myers. *AIChE J*., **2001**, *47*, 1160.
14 A. L. Spek. *ActaCrystallogr*., **1990**, *A46*, C34.
15 V. K. Peterson, Y. Liu, C. M. Brown and C. J. Kepert*J. Am. Chem. Soc*. **2006**, *128*, 15578. (b) C. M. Brown, Y. Liu, T. Yildirim, V. K. Peterson and C. J. Kepert. *Nanotechnology*, **2009**, *20*, 204025
16 (a) K. A. Forrest, T. Pham, K. McLaughlin, J. L. Belof, A. C. Stern, M. J. Zaworotko and B. Space. *J. Phys. Chem. C*, **2012**, *116*, 15538.; (b) T. Pham, K. A. Forrest, P. Nugent, Y. Belmabkhout, R. Luebke, M. Eddaoudi, M. J. Zaworotko and B. Space. *J. Phys. Chem. C*, **2013**, *117*, 9340.; (c) T. Pham, K. A. Forrest, A. Hogan, K. McLaughlin, J. L. Belof, J. Eckert and B. Space. *J. Mater. Chem. A*, **2014**, *2*, 2088.; (d) T. Pham, K. A. Forrest, J. Eckert, P. A. Georgiev, A. Mullen, R. Luebke, A. J. Cairns, Y. Belmabkhout, J. F. Eubank, K. McLaughlin, W. Lohstroh, M. Eddaoudi and B. Space. *J. Phys. Chem. C*, **2014**, *118*, 439.